

# High Tensile Strength Steel Plates and Welding Consumables for Architectural Construction with Excellent Toughness in Welded Joint —“JFE EWEL” Technology for Excellent Quality in HAZ of High Heat Input Welded Joints—<sup>†</sup>

KIMURA Tatsumi<sup>\*1</sup> SUMI Hiroyuki<sup>\*2</sup> KITANI Yasushi<sup>\*3</sup>

## Abstract:

The “JFE EWEL” technology for improving the toughness of heat affected zone (HAZ) effected by high heat input welding has been applied to make SA440 high tensile strength steel plates for architectural constructions. The developed “JFE EWEL” technology consists of minimizing the coarse grain HAZ region through controlling TiN particles, refining the microstructure of HAZ by using BN and Ca inclusions as nucleation sites of intra-granular ferrites and decreasing carbon equivalent ( $C_{eq}$ ) of steel. Furthermore, welding consumables have been newly developed to control the microstructure of HAZ through diffusive B atoms from weld metal to base material. The developed 100 mm thick SA440 grade steel plate exhibits excellent HAZ toughness in welded joints produced by SAW and ESW with high heat inputs. Consequently, JFE Steel has various kinds of high tensile strength steel plate and welding consumable for architectural construction with excellent toughness in welded joint.

## 1. Introduction

Based on the experience of the Hanshin-Awaji Earth-

quake (1995) and other disasters<sup>1)</sup>, high toughness in welded joints in architectural steel frame structures has been strongly required in recent years from the viewpoint of seismic resistance<sup>2)</sup>.

On the other hand, a large number of super-high rise buildings have been constructed or are planned as part of urban revitalization and redevelopment projects. The features of these super-high rise buildings include both large spans and multi-story designs in commercial space, offices, and hotels. As a result, building structures have become more complex, and cases where high tensile forces act on column materials during earthquakes can also be presumed in areas around seismic components and in floors with modified architectural structures<sup>3)</sup>. Therefore, in order to prevent brittle fracture, high toughness has become a requirement not only in column-to-beam welded joints, but also in welded joints in columns<sup>3,4)</sup>.

The column materials used in super-high rise buildings are mainly box columns which are fabricated by welding high tensile strength thick plates with thicknesses exceeding 40 mm. The methods used in welding box columns are submerged arc welding (SAW) and non-consumption type electro slag welding (ESW),

<sup>†</sup> Originally published in *JFE GIHO* No. 5 (Aug. 2004), p. 38–44



<sup>\*1</sup> Senior Researcher Deputy Manager,  
Plate & Shapes Res. Dept.,  
Steel Res. Lab.,  
JFE Steel



<sup>\*2</sup> Senior Researcher Deputy Manager,  
Joining & Strength Res. Dept.,  
Steel Res. Lab.,  
JFE Steel



<sup>\*3</sup> Senior Researcher Deputy Manager,  
Joining & Strength Res. Dept.,  
Steel Res. Lab.,  
JFE Steel

which are high efficiency high heat input welding methods. Because the microstructure of the heat affected zone (HAZ) and the weld metal (WM) coarsens in this type of high heat input welding, reduced toughness had been unavoidable with conventional steels.

JFE Steel carried out research and development of steel plates and welding consumables which make it possible to improve toughness in welded joints, even in this type of high heat input welding<sup>5,6)</sup>, and has now developed a new high performance 590 N/mm<sup>2</sup> steel for architectural construction with a design standard strength of 440 N/mm<sup>2</sup>, together with welding consumables, thus completing a lineup of steel plates and welding consumables for architectural construction with excellent toughness in high heat input welded joints in tensile strengths from 490 N/mm<sup>2</sup> to 590 N/mm<sup>2</sup>.

This paper describes a technology called “JFE EWEL” for realizing high toughness in the high heat input welded joints applied in box columns, the base material performance of a new high performance 590 N/mm<sup>2</sup> steel plate (SA440-E) which was developed using this technology, and the performance of high heat input welded joints using newly developed welding consumables for SAW and ESW.

## 2. Application of High Heat Input Welding to Box Columns and Performance Targets

### 2.1 Changes in HAZ Microstructure Due to Application of High Heat Input Welding and Technical Problems

In fabricating box columns, SAW is applied in corner welding, while ESW is applied in inner diaphragm welding. In actual fabrication, the heat input with these welding methods increases corresponding to increases in the applied plate thickness, and in some cases exceed 60 kJ/mm in SAW and 100 kJ/mm in ESW. **Figure 1** shows a schematic illustration of the changes in the

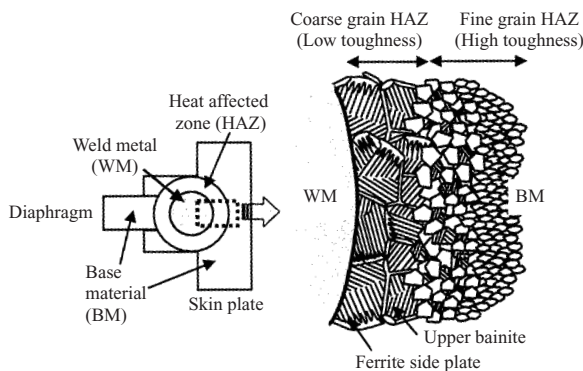


Fig.1 Schematic illustration of HAZ microstructure in large heat input welded joint

Table 1 Aimed properties of steel plates and welded joints

Grade	Base material					Welded joint $\sqrt{E_0}$ (J)
	YP (MPa)	TS (MPa)	YR (%)	El* (%)	$\sqrt{E_0}$ (J)	
HBL325-E	325-445	490-610	≧80	≧21	≧27	≧70
HBL355-E	355-475	520-640	≧80	≧21	≧27	
HBL385-E	385-505	550-670	≧80	≧20	≧70	
SA440-E	440-540	590-740	≧80	≧20	≧47	

\* Test piece : JIS No.4

microstructure of an large heat input welded joint, using inner diaphragm welding (ESW) as an example. Because the HAZ is held for a long period at a high temperature exceeding 1 400°C, the austenite ( $\gamma$ ) grains coarsen remarkably. In the cooling process after welding, the toughness of the HAZ is reduced because coarse ferrite side plates form from the  $\gamma$  grain boundaries during the  $\gamma \rightarrow \alpha$  transformation, while in the former austenite grains, the microstructure changes to upper bainite including martensite/austenite constituent (M-A). In general, high strength, thick steel plates invite an increase in the carbon equivalent ( $C_{eq}$ ), and as a result, HAZ toughness is markedly reduced.

Accordingly, in order to improve HAZ toughness, study from both aspects of minimizing the coarse grain HAZ (CGHAZ) and controlling the intra-granular microstructure is necessary.

### 2.2 Performance Targets

**Table 1** shows the development targets for the base material and welded joints. The target plate performance is the same as the standards for the existing HBL325, HBL355, HBL385, and SA440, which have received material authorization from Japan’s Minister of Land, Infrastructure and Transport. Furthermore, the 0°C Charpy absorbed energy ( $\sqrt{E_0}$ ) of the HAZ, fusion line (FL), and weld metal (WM) in SAW and ESW targeted an average value of 70 J or higher, which is the same as the performance requirement for welded joints in beam edge welds in steel frames when using low heat input multi-layered welding<sup>7)</sup>. It should be noted that the suffix-E added to the standard symbols in Table 1 means a steel plate with high toughness in high heat input welded joints in which “JFE EWEL” is applied.

## 3. High Toughness Technology for High Heat Input Welded Joints in Architectural Construction

### 3.1 Technical Factors of “JFE EWEL”

**Figure 2** shows the technical factors of “JFE EWEL,” which is applied as a technology for improving the

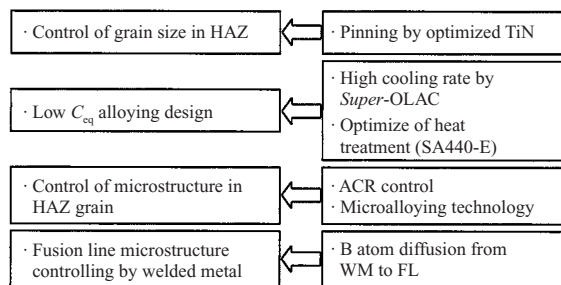


Fig.2 Concepts of "JFE EWEL" technology for improving toughness of welded joints with high heat input welding

toughness of the HAZ in box columns when high heat input welding is performed. This technology is a fusion of four element technologies: (1)  $\gamma$  grain refinement technology, (2) intra-granular microstructure control technology, (3) optimum chemical composition design and production process, and (4) HAZ microstructure control using B dissolution from the WM. By applying these technologies to high tensile strength steel plates for architectural construction, it was possible to improve the toughness of high heat input welded joints.

### 3.2 $\gamma$ Grain Refinement Technology

In minimizing the coarse grain HAZ (CGHAZ), use of stable nitrides and oxides at high temperatures, which suppresses coarsening of  $\gamma$  grains, is effective<sup>5,6,8-12</sup>. Because fine dispersion of TiN in steel can be controlled easily in industrial processes, JFE Steel studied a technology which makes maximum use of the  $\gamma$  grain refinement effect of this nitride.

Based on a thermodynamic analysis using Thermo-Calc and experimental studies, it was possible to increase the dissolution temperature of TiN from the conventional level of less than 1 400°C to more than 1 450°C and to achieve fine dispersion of the TiN by controlling the contents of Ti and N, the Ti/N ratio, and microalloying.

Using a synthetic welding heat cycle device, the  $\gamma$  grains in steel using this  $\gamma$  grain refinement technology were investigated by heating to 1 400°C and slow cool-

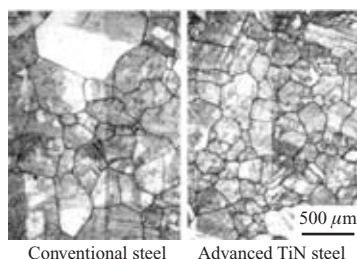


Photo 1 Microstructures of synthetic HAZ of conventional and advanced TiN steels made by heating to 1 400°C followed by quenching

ing to 1 200°C in 80 s, which corresponds to the temperature history of the HAZ during high heat input welding, followed by quenching to freeze the high temperature microstructure. The results are shown in **Photo 1** in comparison with a conventional steel. Because the  $\gamma$  grains were refined to 200  $\mu\text{m}$  or less by applying the  $\gamma$  grain refinement technology, minimization of the CGHAZ can be expected.

### 3.3 Intra-granular Microstructure Control Technology

In order to investigate the effect of the intra-granular microstructure on HAZ toughness, the relationship between the microstructure and changes in synthetic HAZ toughness was investigated using a synthetic welding heat cycle device with steels in which the  $C_{\text{eq}}$  was varied between 0.34 and 0.44%. The material was heated to 1 400°C, corresponding to ESW with a heat input of 100 kJ/mm, and the cooling time from 800°C to 500°C ( $\Delta t_{800-500}$ ) was set at 1 000 s. **Figure 3** shows the effect of the  $C_{\text{eq}}$  on the toughness and hardness of the synthetic HAZ. Steels with a high  $C_{\text{eq}}$  and large quantities of added alloying elements form an upper bainite (UB) microstructure, and the reduction in the toughness of the synthetic HAZ is remarkable. When the  $C_{\text{eq}}$  is reduced, the UB microstructure changes to a ferrite + bainite (F + B) microstructure or ferrite + pearlite (F + P) microstructure, and the toughness of the synthetic HAZ increases. This behavior also corresponds to a reduction in the amount of M-A<sup>5</sup>.

On the other hand, because hardness is reduced corresponding to the changes in the microstructure of the synthetic HAZ, a chemical composition design which considers welded joint strength corresponding to the strength grade becomes necessary. Therefore, in HBL325 steel, the alloy design was prepared so that

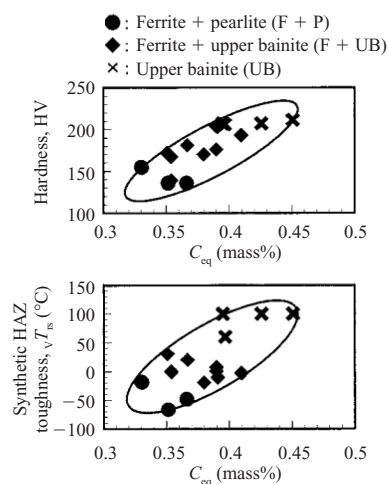


Fig.3 Effect of microstructure on synthetic HAZ toughness and hardness (Reheating cycle: 1 400°C,  $\Delta t_{800-500^\circ\text{C}}$ : 1 000 s)

$C_{eq}$  would be approximately 0.35% in order to achieve an F + P microstructure in HAZ, and in HBL385 and SA440, the alloy design secured  $C_{eq}$  of 0.40% or less to hold F + B microstructure in HAZ, considering welded joint strength.

Furthermore, when necessary, the intra-granular microstructure is refined by using BN and Ca inclusions as nucleation sites for intra-granular ferrite in the  $\gamma \rightarrow \alpha$  transformation<sup>8)</sup>. The function of BN is to reduce free N in the steel, as this is a cause of reduced HAZ toughness. Moreover, BN is also effective in increasing the toughness of the matrix. On the other hand, for effective functioning of Ca inclusions as nuclei for the intra-granular ferrite transformation, proper control of the morphology of the Ca inclusions is necessary. Because strict control of the contents of O, S, and Ca is required to realize this, further improvement in toughness is possible by performing ACR control (ACR: atomic concentration ratio; JFE Steel’s proprietary sulfide morphology control index)<sup>13)</sup>.

### 3.4 Optimal Chemical Composition Design and Production Process

Synthetic HAZ toughness was investigated with HBL325-E steel and SA440-E steel, in which  $\gamma$  grain refinement technology, together with a low  $C_{eq}$  alloy design and ACR control for intra-granular microstructure control, were applied. **Photo 2** shows the microstructure of the synthetic HAZ in which samples were heated to 1 400°C and  $\Delta t_{800-500}$  was set at 1 000 s. The values of  $\sqrt{E_0}$  and hardness are also shown in the photo. The HAZ microstructure of the HBL325 steel is F + P, while that of the SA440 steel is F + B, and  $\sqrt{E_0}$  shows high toughness of the synthetic HAZ, at 339 J and 173 J, respectively.

In manufacturing these newly developed low  $C_{eq}$  steels, with the HBL325 to HBL385 steels, the necessary base material performance is secured by adopting TMCP (thermo-mechanical control process) using JFE Steel’s *Super-OLAC* (on-line accelerated cooling) technology<sup>14)</sup>, which is capable of realizing the theoretical cooling rate in accelerated cooling after rolling. In the

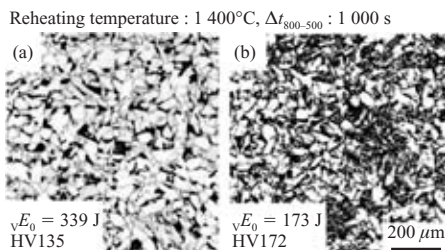


Photo 2 Synthetic HAZ toughness ( $\sqrt{E_0}$ ) and microstructures of the developed steels, (a) HBL325 grade and (b) SA440 grade

SA440 steel, base material performance is secured by adopting a heat treatment process, including reheating and quenching in the  $\gamma + \alpha$  dual-phase region, based on setting and strict control of the proper heat treatment temperature.

### 3.5 HAZ Microstructure Control by B Dissolution from Weld Metal

The CGHAZ is minimized by fine dispersion of high melting point TiN in the steel. However, dissolution of TiN cannot be avoided in the extremely narrow region around the FL, where the temperature exceeds 1 450°C. Thus, there are limits to microstructure control based only on the chemical composition design of the base material. Therefore, JFE Steel studied diffusion of B from the WM, and utilizes this method in improving the toughness of the CGHAZ<sup>15)</sup>. **Figure 4** shows a schematic illustration of behavior of TiN dissolution and B diffusion from high B bearing WM during high heat input welding<sup>8)</sup>. Because TiN dissolves around the FL, there is a danger that free N will have a negative effect on HAZ toughness in this area. For this reason, dissolution of B from the WM is utilized to reduce the content of free N by fixing this free N as BN. In addition, BN can also be employed to control the intra-granular microstructure.

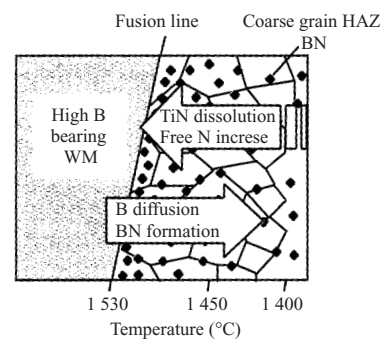


Fig. 4 Schematic illustration for behavior of TiN dissolution and B diffusion from high B bearing WM during high heat input welding

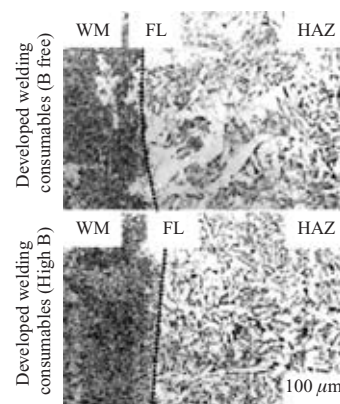


Photo 3 Microstructure of HAZ in welded joints made by using conventional and developed welding consumables

**Photo 3** shows the microstructures of welded joints with ESW welding at a heat input of 100 kJ/mm using the newly developed high-B welding consumable. The material is HBL325-E with  $C_{eq} = 0.34$  mass% and a plate thickness of 60 mm. When the developed welding consumable is used, it can be understood that CGHAZ microstructure in the narrow region around the FL is also refined by diffusion of B from the WM. No similar refinement can be observed with the conventional welding consumables.

#### 4. High Toughness Technology for Weld Metal

With high heat input SAW and ESW, coarsening of the microstructure also occurs in the WM, and as a result, reduced toughness becomes a problem. High toughness in the WM can be achieved by completely suppressing the grain-boundary ferrite which forms at the former  $\gamma$  grain boundaries, as shown in **Fig. 5**, and forming fine acicular ferrite in the grains.

This type of WM microstructure control is possible by proper addition of hardenability elements and elements which suppress grain-boundary ferrite and accelerate the intra-granular acicular ferrite transformation to the welding consumables, and control of the chemical composition of the WM. Because dilution of base metal during welding is on the order of 20–50% in SAW and ESW, it is necessary to consider the effect of the chemical composition of the steel plate when performing WM microstructure control.

Therefore, a detailed composition design was prepared for the welding consumables, assuming an amount of dilution of the base material corresponding to the

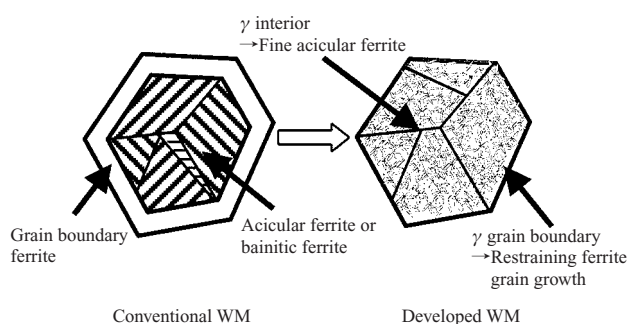


Fig. 5 Schematic illustration of WM microstructure for improving toughness of high heat input welded joint

welding method and its heat input, thereby optimizing the WM microstructure and realizing high toughness in the WM.

Thus, welding consumables for SAW and ESW were developed, matched to the steel plates in which the "JFE EWEL" technology is applied.

#### 5. Development of High Tensile Strength Steel Plate (SA440C-E) with Excellent Toughness in High Heat Input Welded Joints

Steel plates in which the "JFE EWEL" technology is applied were manufactured, and their base material performance and weldability and the performance of SAW and ESW welded joints using the developed welding consumables were studied. Because HBL325-E, 355-E, and 385-E are discussed in separate reports<sup>5,6</sup>, this paper will describe the result of high performance steel plate (SA440-E), centering on test production and the performance of the base material and welded joints.

##### 5.1 Chemical Composition and Manufacturing Conditions of Steel Plates

The developed steel was melted in an actual process, and a slab was produced by continuous casting. **Table 2** shows the typical chemical composition. The carbon content was set at 0.08 mass%, and the alloy composition was optimized considering the hardenability of the plates, by varying the Ni content corresponding to the plate thickness, etc.,  $C_{eq}$  was set at 0.40 mass% or less. To control the HAZ microstructure, Ti and N were strictly controlled and ACR control was performed.

After reheating this slab, plate rolling was performed to produce plates with thicknesses of 60 mm and 100 mm, and heat treatment was performed, including reheating and quenching treatment in the  $\gamma + \alpha$  dual-phase region.

##### 5.2 Mechanical Properties of Plates

**Table 3** shows the mechanical properties of the base material. With both the 60 mm and 100 mm thicknesses, the plates amply satisfy the target base material performance. **Photo 4** shows the microstructure at the 1/4t position in the 100 mm thick plate. By optimizing the

Table 2 Chemical compositions of developed steel plates, SA440-E

Thickness (mm)	(mass%)							
	C	Si	Mn	P	S	Others	$C_{eq}$ (WES)*	$P_{CM}$ **
$t \leq 60$	0.08	0.22	1.58	0.002	0.001	Cu, Ni, Ti, etc.	0.38	0.22
$60 < t \leq 100$	0.08	0.21	1.53	0.008	0.002	Cu, Ni, Ti, etc.	0.38	0.22

\*  $C_{eq}$  (WES) = C + Si/24 + Mn/6 + Ni/40 + Cr/5 + Mo/4 + V/14

\*\*  $P_{CM}$  = C + Si/30 + Mn/20 + Cu/20 + Ni/60 + Cr/20 + Mo/15 + V/10 + 5B

Table 3 Mechanical properties of developed steel plates, SA440-E

	Thickness (mm)	Position	Direction	Tensile properties				Charpy impact test			Reduction of area obtained by Z-direction test (%)
				YP (N/mm <sup>2</sup> )	TS (N/mm <sup>2</sup> )	YR (%)	El (%)	Position	Direction	vE <sub>0</sub> (J)	
Target	19–100	1/4t	C	440–540	590–740	≧ 80	≧ 20	1/4t	C	≧ 47	≧ 25 (Each ≧ 15)
Developed thick plates	60	1/4t	C	470	643	73	30	1/4t	C	221	72 (73, 72, 70)
		1/2t	C	462	637	73	26	1/2t	C	215	
	100	1/4t	C	478	660	72	28	1/4t	C	225	62 (64, 61, 60)
		1/2t	C	466	646	72	22	1/2t	C	183	

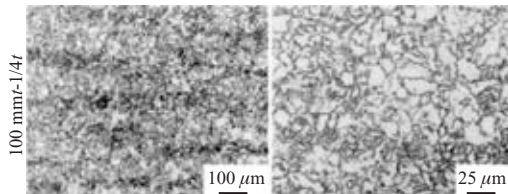


Photo 4 Typical microstructures of developed thick plates

alloy design and reheating and quenching treatment in the  $\gamma + \alpha$  dual-phase region, the base material microstructure achieved a dual-phase structure consisting of a soft phase of ferrite and a hard phase of tempered martensite. As a result, both high strength and a low yield ratio of 80% or less are realized even with a plate thickness of 100 mm. Toughness, ductility, and reduction of area in the plate thickness direction also amply satisfied the targets.

5.3 Welded Joint Performance

To investigate the welded joint toughness improvement effect, corner welds and inner diaphragm welded joints were produced by SAW and ESW, respectively, using developed plates 60 mm in thickness and the developed welding consumables.

5.3.1 Welding conditions and microstructure

Table 4 shows the groove shape and welding conditions. High heat input welding was performed in SAW with tandem electrodes ((2 electrodes)/(1 run)) at a heat input of 63 kJ/mm. The heat input in ESW was 100 kJ/mm. The welding consumables for SAW and ESW were described in the previous chapter. Welding wire and flux were used considering also the effect of base material dilution during welding on the WM and microstructure control of the FL.

Photo 5 shows the macrostructure of the welded joints and the microstructure of the WM. The bead shape is satisfactory and adequately penetrates the base mate-

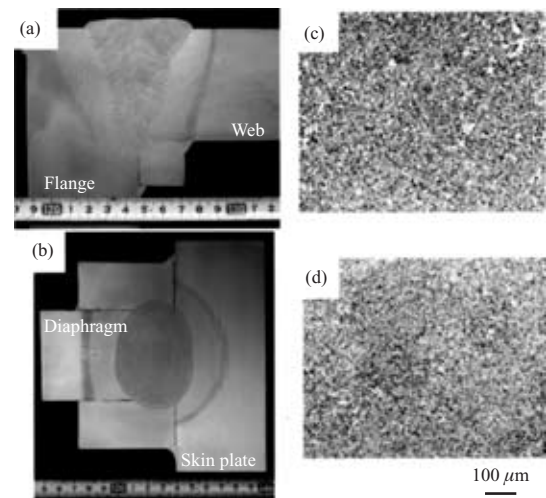


Photo 5 Macrostructures of (a) SAW, (b) ESW welded joints and WM microstructures of (c) SAW, and (d) ESW welded joints

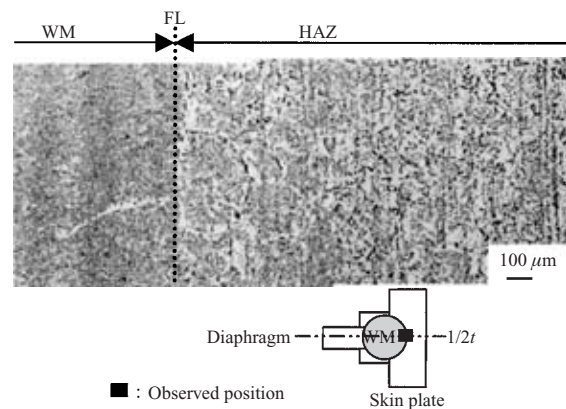


Photo 6 Microstructure of ESW welded joint

Table 4 Welding conditions for evaluation of welded joint toughness

Welding method	Electrode (Diameter)	Flux	Current (A)	Voltage (V)	Speed (mm/min)	Heat input (kJ/mm)	Pass	Groove shape	Plate Thickness (mm)
SAW (Tandem electrode)	L	KW-55	2 300	40	180	63	1	Y shape	60
	T	KB-55I AD	1 800	53					
ESW	KW-60 AD (φ1.6 mm)	KF-100 AD	380	52	11.8	100	1		Skin plate : 60 Diaphragm : 60

rial, and no harmful welding defects were found. In the macrostructure, minimization of the CGHAZ has been realized, with no remarkable coarse grains observed. The microstructure of the WM has formed the targeted fine acicular ferrite, and formation of coarse ferrite at the former  $\gamma$  grain boundaries could not be detected.

**Photo 6** shows an example of the HAZ microstructure on the skin plate side of an ESW welded joint. The HAZ consists of the targeted fine F + B microstructure, and the intra-granular microstructure of the CGHAZ which can be seen in an extremely narrow region around the FL has been refined by ACR control of the plate and B dissolution from the WM.

### 5.3.2 Welded joint toughness

**Table 5** shows the Charpy impact properties of the WM, FL, and HAZ 3 mm position in SAW and ESW welded joints. In the SAW and ESW, Charpy absorbed energy at 0°C showed the targeted value of 70 J or higher at all positions, including the WM, FL, and HAZ.

### 5.3.3 Welded joint tensile properties

To investigate the strength of welded joints produced by high heat input welding, cross-shaped welded joints were produced and tensile tests for welded joints were performed with SAW welded joints and joints

between the inner diaphragm and skin plate, and beam. In the cross-shaped welded joints, the developed steel with a thickness of 60 mm was used as the skin plate, and the developed steel with the thickness reduced to 50 mm was used as the diaphragm and beam material. The skin plate and inner diaphragm were welded by ESW, and CO<sub>2</sub> multi-layered welding at a heat input of 1.3 to 2.2 kJ/mm was performed in welding the skin plate and beam. In SAW and ESW, welding was performed under the same conditions as in Table 4.

**Table 6** shows the results of the tensile test for welded joints. Fracture in the SAW welded joint and cross-shaped welded joint occurred in the HAZ and in the HAZ on the diaphragm side, respectively. However, the strength of the respective welded joints was 611 N/mm<sup>2</sup> and 658 N/mm<sup>2</sup>, satisfying the target of 590 N/mm<sup>2</sup> or higher.

## 6. Conclusion

This paper has described "JFE EWEL," which is an HAZ microstructure control technology for achieving high toughness in welded joints in high heat input welding by SAW and ESW, and the base material performance and performance of high heat input welded joints of newly developed SA440-E steel plates using the developed welding consumables. By applying this technology to high tensile strength steel plates for architectural construction, high toughness was realized in welded joints in high heat input welding by SAW and ESW methods.

In order to meet diverse customer needs, JFE Steel provides a full lineup of high tensile strength steel plates for architectural construction with excellent toughness in high heat input welded joints, in tensile strengths ranging from 490 N/mm<sup>2</sup> to 590 N/mm<sup>2</sup>, as well as SAW and ESW welding consumables for these plates. Lists of these high tensile strength steel plates and the

Table 5 Results of V-notch Charpy impact test of welded joints

Joint type	Position	Notch position	Charpy absorbed energy, $\sqrt{E_0}$		
			HAZ (J)	FL (J)	WM (J)
SAW	Web side	2 mm from surface	247*	165	95
	Flange side		123*	132	
ESW	Skin plate side	2 mm from surface	185*	92	78
		1/2t	210*	98	100

\* 3 mm from fusion line  
FL : Fusion line

Table 6 Results of tensile test for welded joints

Welded joint type	TS (N/mm <sup>2</sup> )	Fracture position	Illustration of tensile test specimen
SAW welded joint (according to JASS 6)	611	HAZ	
Diaphragm-column-beam flange cross-shaped welded joint (according to JASS 6)	658	HAZ of diaphragm side	

unit : mm

Table 9 List of JFE Steel’s steel plates for architectural construction

Standard	Class	Symbol	Standard	Class	Symbol
Standard for material authorization, Minister of Land, Infrastructure and Transport	TMCP steel for architectural construction	HBL352B, 325C HBL355B, 355C	JIS standard	Rolled steel for architectural construction (JIS G 3136)	SN400A, 400B, 400C SN490B, 490C
	550 N/mm <sup>2</sup> TMCP steel of architectural construction	HBL385B, 385C	Fireproof steel standard	Fireproof steel for architectural construction	SN400B-FR, 400C-FR SM400B-FR, 400C-FR SN490B-FR, 490C-FR SM490B-FR, 490C-FR HBL325B-FR, 325C-FR SM520B-FR HBL355B-FR, 355C-FR
	High-performance 590 N/mm <sup>2</sup> grade steel for building structures	SA440B, 440C SA440B-U, 440C-U			
	Low yield point steel for architectural construction	JFE-LY100 JFE-LY160 JFE-LY225			

Table 7 List of high strength steel plates with excellent toughness for high heat input weld joints

Strength class of plate	Symbol	Corresponding standard and applicable thicknesses
490 N/mm <sup>2</sup>	SN490CTMC-E HBL325C-E	JIS G 3136, 19 – 40 mm Authorized products, 40.1–100 mm
520 N/mm <sup>2</sup>	HBL355C-E	Authorized products, 40.1–100 mm
550 N/mm <sup>2</sup>	HBL385C-E	Authorized products, 19 –100 mm
590 N/mm <sup>2</sup>	SA440C-E	Authorized products, 19 –100 mm

Table 8 List of welding consumables with excellent toughness for high heat input weld joints

Strength class of welding consumables	Welding wire		Flux	
	Brand	JIS standard	Brand	JIS standard
SAW	490–520 N/mm <sup>2</sup>	KW-55	Z 3351 YS-M1	KB-55I AD Z 3352 FS-BT1
	550–590 N/mm <sup>2</sup>	KW-101B + KW-55	Z 3351 YS-NM1 + Z 3351 YS-M1	KB-60I AD Z 3352 FS-BT1
ESW	490–590 N/mm <sup>2</sup>	KW-60AD	Z 3353 YES 62	KF-100 KF-100AD Z 3353 FS-FG3

corresponding welding consumables are presented in **Tables 7 and 8**, respectively. Finally, a list of JFE Steel’s steel plates for architectural construction by standard is shown in **Table 9**.

**References**

- 1) How far was the fracture phenomenon of a steel frame solved? The present measure technology. Panel-discussion data. Structure Section of AIJ Convention, Structure Committee of Architectural Institute of Japan (AIJ). 2000.
- 2) Toyoda, M. “Earthquake resistance and welding of steel structure framework.” Jpn. Welding Engineering Soc. Symp. no. 10, 1998, p. 97–99.
- 3) Inada, T.; Ogawa, I. CAMP-ISIJ. vol. 16, 2003, p. 340–343.
- 4) Inada, T. The Structural Technology. no. 8, 2001, p. 32.
- 5) Kimura, T.; Hisada, M.; Fuzisawa, S.; Yokoyama, Y.; Katori, S. Kawasaki Steel Giho. vol. 34, no. 4, 2002, p. 158–163.
- 6) Hayashi, K.; Nakagawa, I.; Fuzisawa, S. JFE Technical Report. no. 5 2004, p. 53–59.
- 7) The Brittle-Like Fracture Prevention Guideline of a Steel Frame Beam Edge Welded Joint and This Description. Jpn. Building Soc. 2003-09.
- 8) Suzuki, S.; Oi, K.; Ichimiya, K.; Kitani, Y.; Murakami, Y. Materia. vol. 43, no. 3, 2004, p. 232–234.
- 9) Funakoshi, T.; Tanaka, T.; Ueda, S.; Ishikawa, M.; Koshizuka, N. Tetsu-to-Hagané. vol. 63, no. 2, 1977, p. 303.
- 10) Deshimaru, S.; Hirai, M.; Amano, K. Kawasaki Steel Giho. vol. 18, no. 4, 1986, p. 295.
- 11) Nishimori, M.; Hayashi, T.; Kawabata, F.; Amano, K. CAMP-ISIJ. vol. 10, 1997, p. 592.
- 12) Kasamatsu, Y.; Takashima, S.; Hosotani, R. Tetsu-to-Hagané. vol. 65, no. 8, 1979, p. 12–22.
- 13) Haida, O.; Emi, T.; Kawanishi, G.; Naitou, M.; Moriwaki, S. Tetsu-to-Hagané. vol. 66, 1980, p. 354–362.
- 14) Omata, K.; Yoshimura, H.; Yamamoto, S. NKK Technical Review. no. 88, 2003, p. 73–80.
- 15) Kitani, Y.; Ikeda, R.; Oi, K.; Ichimiya, K. Preprints of the National Meeting of Jpn. Welding Soc. vol. 72, 2003, p. 108–109.